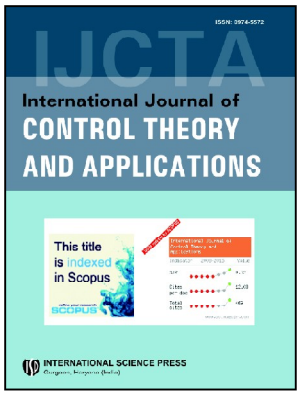

International Journal of Control Theory and Applications

ISSN : 0974-5572

Volume 10 • Number 11 • 2017

Thermal Properties of Al_2O_3-water nanofluids to examine heat transfer enhancement in heat exchangers

Paideti Lavanya Sarala[1] and B. Nageswara Rao[2]

Department of Mechanical Engineering, K L University, Green Fields, Vaddeswararam, Guntur 522502, India
[1]E-mail: paidetilavanya@gmail.com
[2]Corresponding author, E-mail: bnrao52@rediffmail.com;bnrao52@kluniversity.in

Abstract: Nanofluids are made by mixing Al_2O_3 nanoparticles to water with different volume concentrations, whose properties (viz., thermal conductivity, viscosity, specific heat and density) are evaluated at different temperatures. Performance of a typical one pass square pitch shell and tube heat exchanger has been examined using distilled water and hot nanofluids in shell and tube respectively. The overall heat transfer coefficient and pressure drop are estimated to demonstrate the heat transfer enhancement using nanofluids in heat exchangers.

Keywords: Thermal conductivity; dynamic viscosity; nanofluids; shell and tube heat exchanger; pressure drop; overall heat transfer coefficient.

1. INTRODUCTION

Heat transfer fluids (such as water, mineral oil and ethylene glycol) are being used in many industrial sectors including power generation, chemical production, air-conditioning, transportation and microelectronics. However, performance of these conventional heat transfer fluids is limited due to low thermal conductivity. High performance heat transfer fluids are required to meet the demands of industries for process intensification and device miniaturization.

At room temperature, metals possess very high thermal conductivity when compared to that of fluids. The ratio of thermal conductivity of copper to water is about 700, whereas it is 3000 for engine oil in place of water. The thermal conductivity of fluids containing suspended metallic or nonmetallic (metallic oxide) particles is expected to be higher than that of conventional heat transfer fluids. Particles clogging, sedimentation and erosion are some of the common problems associated with the use of micro or millimeter sized solid particles when suspended in the host fluids. Such problems can be minimized by changing micrometer sized particles to nano-sized particles.

Experimental studies on nanofluids are confined to laminar /turbulent flow conditions in which the mixed base fluid is water. In severe cold climatic conditions glycols are mixed to water to reduce the freezing point of heat transfer liquids. Glycol based fluids are used in base board heaters, automobile radiators and process plants

mainly in cold countries where the ambient temperature is below 0^0C. Nano particles used in nanofluids are oxide ceramics (Al_2O_3, CuO, Cu_2O), nitride ceramics (AlN, SiN), carbide ceramics (SiC, TiC), metals (Ag, Au, Cu, Fe), semiconductors (TiO_2), single or double or multi-walled carbon nano tubes (SWCNT, DWCNT, MWCNT), and composite materials such as nanoparticle core-polymer shell composites.

The base fluids used in nanofluids are water, engine oil, ethylene glycol and ethanol. Nanofluids are made by two-step process (i.e., preparation of nanoparticles and later on dispersion into the base fluid), single step process (i.e., preparation and simultaneous dispersion of nanoparticles into base fluids), and other processes. In single step process, the processes of drying, storage, transportation, and dispersion of nanoparticles can be avoided, which minimizes agglomeration of nanoparticles and increases the stability of fluids. However, it is a slow process and is expensive at industrial scale. Processes such as templating, micro-droplet drying, electrolysis metal deposition, layer-by-layer assembly and other colloid chemistry techniques are suitable to nano particles with specific porosities, densities, geometries, charge, and surface chemistries.

Lee *et al.* [1], Das *et al.* [2], Xuan *et al.* [3], and Ebrahimi *et al.* [4] have examined the properties of nanofluids containing metals and metal oxides nano particles. This paper examines the properties of nanofluids by mixing Al_2O_3 nano particles to water at different temperatures. The heat transfer enhancement using such nanofluids in heat exchangers is demonstrated by estimating the overall heat transfer coefficient and the pressure drop.

2. PREPARATION OF AL_2O_3- WATER NANOFLUIDS

Nanofluids are prepared using Al_2O_3 nano particles procured from a USA based company, Sigma-Aldrich Chemicals Private Ltd., Bangalore. The procured product is the Alumina Powder Nano Grade (99.99% Al_2O_3content) possessing white colour, Alpha crystal form with 6.6 PH value. The other specifications of the product are: Si=10.8ppm; Na=9.01ppm; K=10.6ppm; Fe=9.75ppm; Cu=0.12ppm; Ti=0.86ppm; and Mn=0.72ppm. The diameter of the nanoparticle (d_p) and the specific surface are44nm and15m^2/g, respectively. Thermal properties of nano particles (in solid form) are: thermal conductivity, k_p=40W/m-K; thermal conductivity of interfacial layer, k_{layer} =3.2 W/m-K; specific heat of nano particles, C_{p_p} = 0.765KJ/kg.K; interfacial layer of nano layer thickness, t=2nm; packing fraction of water, m=2.5; and maximum particle concentration, ϕ_m = 5.5 at pressure of 1 atm. These nanoparticles are mixed with water and expected negligible change in properties due to water temperature. Table-1 gives the properties of the base fluid (water) at the specified temperatures. The amount of Al_2O_3 nano particles for preparation of nanofluids is arrived from the law of mixture.

Volume concentration factor,

$$\phi = \frac{w_p}{\rho_p}\left(\frac{w_p}{\rho_p}+\frac{w_f}{\rho_f}\right)^{-1} \tag{1}$$

Here w_p and w_f are the weights of nanoparticles and base fluid (water) respectively. ρ_p And ρ_f are the corresponding densities. The weight of the nano particles for the specified ϕ from equation (1) can be obtained as

$$\frac{w_p}{\rho_p}(1-\phi)=\phi\left(\frac{w_f}{\rho_f}\right)\Rightarrow w_p=\rho_p\left(\frac{w_f}{\rho_f}\right)\left(\frac{\phi}{1-\phi}\right) \tag{2}$$

The density of the nanoparticles, ρ_p = 3970kg/m^3 and the density of water at room temperature (25^0C), ρ_f= 1000kg/m^3. To measure the properties of Al_2O_3- water nanofluids at room temperature (25^0C), 19.9 grams of nanoparticles are required for volume concentration, ϕ = 0.1to mix in 5 liters of water. Similarly 9.96 grams of

nanoparticles are used for volume concentration, $\phi = 0.05$ and 4.98 grams of nanoparticles are used for volume concentration, $\phi = 0.025$. Table 2 provides the weight of nanoparticles (w_p) to mix in 5 liters of water at 60,70 and80^{0}C.A sensitive balance with 0.1mg resolution is used to weigh the Al_2O_3 nanoparticles. A small amount (i.e., one–tenth of the mass of nano particles) of surfactant (viz., Sodium Dodecyl Benzene Sulfonate) is added in Al_2O_3-water nanofluid and stirred for five hours for a stable suspension with uniform particle dispersion in the water, to prevent from the corrosion of the tube material.Figure-1 shows the mixing of the specified volume concentration of Al_2O_3nanoparticles to water. Al_2O_3-water nanofluids having volume concentrations, $\phi = 0.025$, 0.5 and 0.1 are prepared without any particle settlement at the bottom of the tank. Properties of isentropic Newtonian Al_2O_3-water nanofluids are evaluated at temperatures of 60, 70, and 80^{0}C.

Table 1
Water properties at the specified temperature (T)

Properties	*T=30^{0}C*	*T=50^{0}C*	*T=60^{0}C*	*T=70^{0}C*	*T=80^{0}C*
Thermal conductivity, k_f(W/m-K)	0.612	0.6396	0.6513	0.66	0.6687
Specific heat, C_{p_f}(kJ/kg.K)	4.178	4.180	4.183	4.189	4.195
Density, ρ_f(kg/m^3)	997.5	990	985	979.5	974
Viscosity, μ_f($\times 10^{-4}$) (kg/m.s)	8.294	5.381	4.708	4.126	3.545
Prandtl number, *Pr*	5.68	3.68	3.020	2.62	2.220

Table 2
Weight of the nanoparticles, w_p (gms) for the specified volume concentration (ϕ) to mix in 5 litres of water at the specified temperatures

ϕ	*T=60^{0}C*	*T=70^{0}C*	*T=80^{0}C*
0.025	5.04	5.07	5.10
0.05	10.09	10.15	10.21
0.1	20.21	20.3	20.4

3. EXPERIMENTAL SETUP

The test setup in Figure 2 consists of radiator, fan, flow meter, pump, two thermocouples, and a tank with heating element. The size of the radiator is 450×385×3mm, which consists of corrugated shape fin with 1.14 liters capacity. Tubes and fins are made of aluminum.

3.1. Testing Procedure

The heating element in the test apparatus will be acting as a source of heat (just like an engine in an automobile), which will heat up the coolant in the temperature range of 60-80ºC. After heating, the hot water is pumped with the help of a pump in to the radiator. At the outlet of the pump a flow meter is installed to measure the mass flow rate. The flow is controlled by a valve. The inlet temperature is measured by installing a thermocouple with digital meter. The hot fuel flows through the radiator. Cold air is sucked-in with a fan to reduce the temperature of the coolant flowing through the radiator. The temperature at outlet is measured by another thermocouple. Later on, the coolant from outlet is returned to the reservoir where it becomes hot by the heating element and re-circulates in the flow circuit to maintain the continuity of flow.

Initially water is taken as a coolant and circulated at different mass flow rates (4, 6& 8 liters per minute). The fan is on with 2300 rpm. The temperature of the inlet coolant is maintained at 60, 70 and 80ºC and recorded the corresponding temperature of hot coolant at the outlet. This process is repeated by changing water to Al_2O_3 – water nanofluids.

Figure 1: Mixing of Al_2O_3 nanoparticles to water

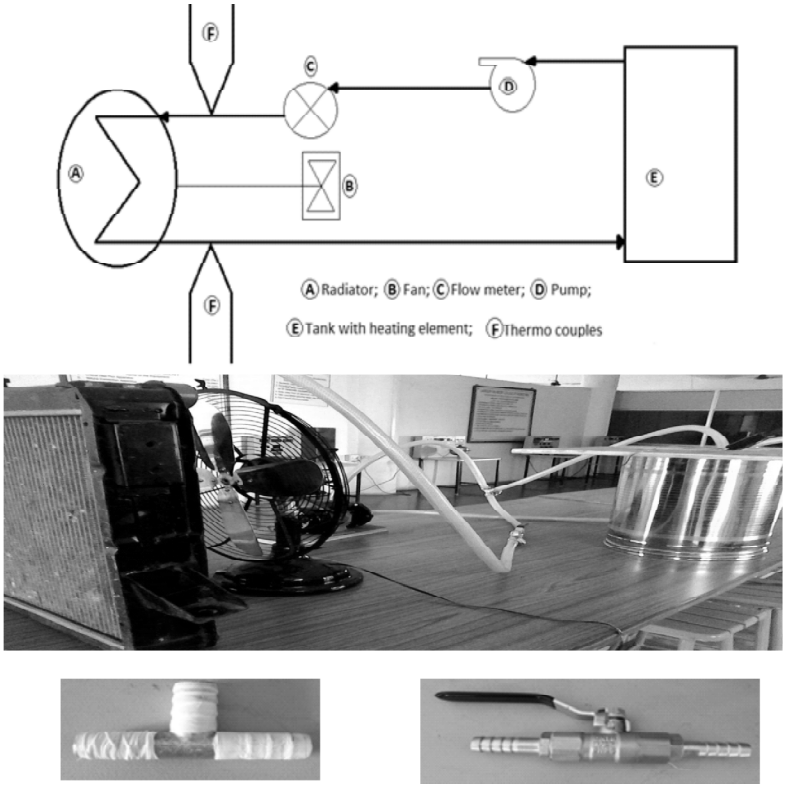

Figure 2: Experimental setup including the use of Control valve and T-joint in fabrication

3.2. Properties of Al_2O_3–water nanofluids

The heat transfer characteristics of nanofluids are examined by evaluating their thermo-physical properties such as density, specific heat, viscosity and thermal conductivity.

3.2.1. Empirical relations for density and specific heat

The density (ρ_{nf}) of Al_2O_3-water nanofluids for the volume concentration (ϕ) is measured by using hygrometer. The empirical relation of Ebrahimi [4] as a function of the density of base fluid (ρ_f) and that of nanoparticles (ρ_p) is

$$\rho_{nf} = (1-\phi)\rho_f + \phi\rho_p \tag{3}$$

The specific heat ($C_{p_{nf}}$) of the nanofluids can be obtained for the volume concentration (ϕ) using the specific heat of base fluid (C_{pf}) and that of nanoparticles (C_{p_p}) from the empirical relation

$$C_{pnf} = \frac{1}{\rho nf}\left\{(1-\phi)C_{pf}\rho_f + \phi C_{p_p}\rho_p\right\} \tag{4}$$

3.2.2. Empirical relations of effective thermal conductivity (k_{eff})

Several empirical relations are developed for the effective thermal conductivity (k_{eff}) in terms of the thermal conductivity of nanoparticles (k_p) and that of the base fluid (k_f) [5-15]. A few of the frequently used Maxwell, Bruggeman *et al.,* Hamilton and Crosser, Jeffrey empirical relations [5] along with those of Xuan *et al.* [6] and Corcione [7] are presented below.

$$\text{Maxwell: } \frac{k_{eff}}{k_f} = \frac{k_p + 2k_f + 2(k_p - k_f)\phi}{k_p + 2k_f - (k_p - k_f)\phi} \tag{5}$$

$$\text{Bruggeman } et\ al.\text{: } \frac{\phi(k_p - k_{eff})}{k_p + 2k_{eff}} + (1-\phi)\frac{(k_f - k_{eff})}{k_f + 2k_{eff}} = 0 \tag{6}$$

$$\text{Hamilton and Crosser: } \frac{k_{eff}}{k_f} = \frac{k_p + (n-1)k_f + (n-1)(k_p - k_f)\phi}{k_p + (n-1)k_f + (k_f - k_p)\phi} \tag{7}$$

Here n is the shape factor, which is equal to 3 for spherical particle.

$$\text{Jeffrey: } \frac{k_{eff}}{k_f} = 1 + 3\eta\phi + \phi^2\left\{3\eta^2 + \frac{3\eta^2}{4} + \frac{9\eta^3}{16}\frac{(k+2)}{(2k+3)} + \ldots\right\}, \tag{8}$$

in which, $k = \frac{k_p}{k_f}$ *and* $\eta = \frac{k-1}{k+2}$.

$$\text{Xuan } et\ al.\text{: } k_{nf} = \frac{k_p + 2k_f - 2(k_f - k_p)\phi}{k_p + 2k_f + (k_f - k_p)\phi}k_f + \frac{\rho_p\phi C_{p_p}}{2}\sqrt{\frac{k_B T}{3\pi r_c \mu_f}}, \tag{9}$$

Where is the mean radius of gyration of the cluster, μ_f is dynamic viscosity of the base fluid, T is the temperature, and $k_B = 1.3807 \times 10^{-23}$, is the Boltzmann constant.

Corcione:
$$\frac{k_{eff}}{k_f} = 1 + 4.4\,\mathrm{Re}^{0.4}\,\mathrm{Pr}^{0.66}\left(\frac{T}{T_{fr}}\right)^{10}\left(\frac{k_p}{k_f}\right)^{0.03}\phi^{0.66}, \tag{10}$$

where Reynolds number, $Re = \dfrac{2\rho_f k_B T}{\pi \mu_f^2 d_p}$.

3.2.3. Empirical relations of effective dynamic viscosity (μ_{eff})

Khanfer and Vafai [5] have used empirical relations of Einstein, Brinkman, Bachelor, Lundgren, Eilers, Saito and Maiga for the effective dynamic viscosity (μ_{eff}) of nanofluids. Vajjha *et al.* [14] have used another empirical relation for μ_{eff}. Tiwari *et al.* [15] have included the empirical relations of Nielson, Krieger and Dougherty as well as Corcine. These are presented below for comparison with test results.

$$\text{Einstein}: \frac{\mu_{eff}}{\mu_f} = (1 + 2.5\phi), \tag{11}$$

Which is developed for low volume concentration of particles ($\phi < 0.01$).

Brinkman:
$$\frac{\mu_{eff}}{\mu_f} = \frac{1}{(1-\phi)^{2.5}} \tag{12}$$

Equation (12) is extension of the Einstein empirical relation (11) for higher volume concentration of particles.

Bachelor:
$$\frac{\mu_{eff}}{\mu_f} = (1 + 2.5\phi + 6.5\phi^2), \tag{13}$$

which is developed by considering the effect of Brownian motion of rigid and spherical particles.

Lundgren:
$$\frac{\mu_{eff}}{\mu_f} = \frac{1}{(1-2.5\phi)} \tag{14}$$

Eilers:
$$\frac{\mu_{eff}}{\mu_f} = 1 + \frac{2.5\phi}{\left(1 - \frac{\phi}{0.78}\right)} \tag{15}$$

Saito:
$$\frac{\mu_{eff}}{\mu_f} = 1 + \frac{2.5\phi}{(1-\phi)} \tag{16}$$

Maiga:
$$\frac{\mu_{eff}}{\mu_f} = (1 + 7.3\phi + 123\phi^2) \tag{17}$$

Vajjha et al.:
$$\frac{\mu_{eff}}{\mu_f} = A_2(\exp(C_2\phi)), \tag{18}$$

where $A_2 = 0.983; C_2 = 12.959;$ *for* $293 \le T \le 363$ *and* $0.01 \le \phi \le 0.1$

Nielsen:
$$\frac{\mu_{eff}}{\mu_f} = (1 + 1.5\phi)e^{\frac{\phi}{1-\phi m}} \tag{19}$$

Krieger and Dougherty:
$$\frac{\mu_{eff}}{\mu_f} = \left(1 - \frac{\phi}{\phi_m}\right)^{-\eta\phi_m}, \tag{20}$$

Here ϕ_m is the maximum packing fraction and η is the intrinsic viscosity. η = 2.5 for hard spheres. For randomly mono-dispersed spheres, $\phi_m \approx 0.64$.

Corcione:
$$\frac{\mu_{eff}}{\mu_f} = \left(1 - 34.87\left(\frac{d_p}{d_f}\right)^{-0.3}(\phi)^{1.03}\right)^{-1}, \tag{21}$$

where, $d_f = 0.1\left(\frac{6M}{N\pi\rho_{fo}}\right)^{\frac{1}{3}}$, is the equivalent diameter of a basefluid molecule, in which molecular weight of the base liquid, M = 18.0152891moles; Avogadro number, N = 6.022×1023; and ρ_{fo} = 998kg/m3 is the mass density of the base fluid (water) at temperature T_0 = 293K. Nguyen *et al.* [13] have performed experiments and measured viscosity of Al_2O_3-water nanofluid. It is customary to examine the adequacy of the empirical relations to generate the properties of nanofluid prior to their use in the performance evaluation of heat exchangers [16].

In order to examine the accuracy of the above empirical relations for the effective thermal conductivity (k_{eff}) and the effective dynamic viscosity (μ_{eff}), experimental results [15] of Al_2O_3-water nanofluids at 50 °C are considered. Table 3 gives a comparison of experimental and estimated? (k_{eff}) of Al_2O_3-water nanofluids at 50 °C. Figure 3 shows a comparison of thermal conductivity? (k_{eff}) of Al_2O_3-water nanofluids at 50 °C with volume concentration (ϕ). Figure 4 shows variation of thermal conductivity with volume concentration (ϕ) for different nanoparticle diameters (10-50nm). The effective thermal conductivity of the Corcione empirical relation (10) is matching well with experimental results. Figure 5 shows variation of thermal conductivity with temperature for the specified volume concentration (ϕ). It is noted that the effective thermal conductivity of the Al_2O_3-water nanofluid decreases with increasing the diameter of the nano particles and increases with increasing temperature. The trend of effective dynamic viscosity (μ_{eff}) evaluated from the Corcione empirical relation (21) is comparable with that of test results in Table 4. To match with results, a multiplication factor α is introduced in the Corcione empirical relation (21) and modified it as

Table 3
Comparison of estimated effective thermal conductivity, k_{eff} (W/m-K) of Al_2O_3-water nanofluids with test data [15] at 50^{0}C

	Maxwell Eq.(5)	*Bruggeman Eq.(6)*	*Hamilton and Crosser Eq.(7)*	*Corcione Eq.(10)*	*Test [15]*
0.025	0.6856	0.6875	0.6856	0.8010	0.8058
0.05	0.7368	0.7464	0.7374	0.8946	0.9082
0.1	0.8314	0.8890	0.8346	1.0426	—

Table 4
Comparison of estimated effective dynamic viscosity, ($\times 10^{-4}$, N-s/m^2) of Al_2O_3-water nanofluids with test data [13, 15] at 50^{0}C

	Model	*$\phi = 0.025$*	*$\phi = 0.05$*	*$\phi = 0.1$*
Einstein	Eq.(11)	5.716	6.052	6.725
Brinkman	Eq.(12)	5.732	6.116	7.001
Batchelor	Eq.(13)	5.738	6.139	7.074
Lundgren	Eq.(14)	5.738	6.148	7.173
Eilers	Eq.(15)	5.727	6.098	6.922
Saito	Eq.(16)	5.725	6.088	6.874
Vajjha	Eq.(18)	7.635	10.556	20.181
Nielsen	Eq.(19)	5.983	6.645	8.168
Krieger	Eq.(20)	5.734	6.127	7.060
Corcione	Eq.(21)	6.931	9.164	26.776
Modified Corcione	Eq.(22)	6.090	7.360	13.879
Test [13,15]		6.460	7.640	—

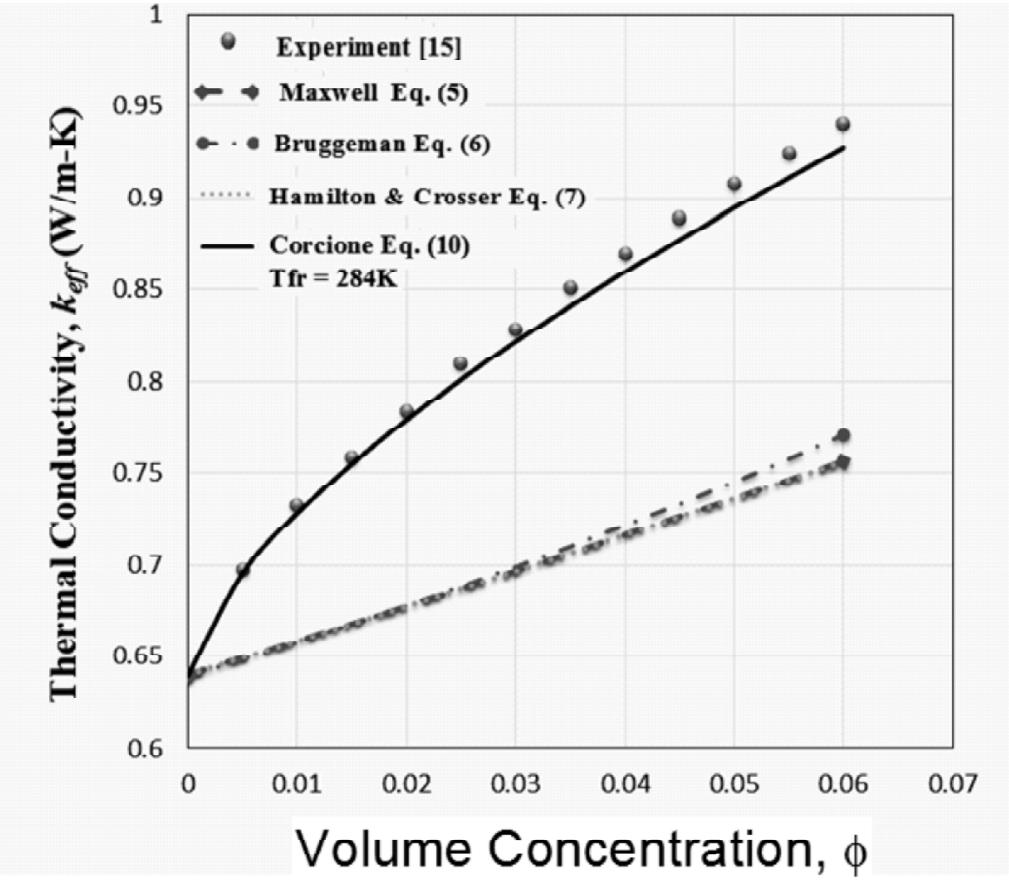

Figure 3: Comparison of thermal conductivity, k_{eff} (W/m – K) of Al_2O_3-water nanofluids with volume concentration, ϕ

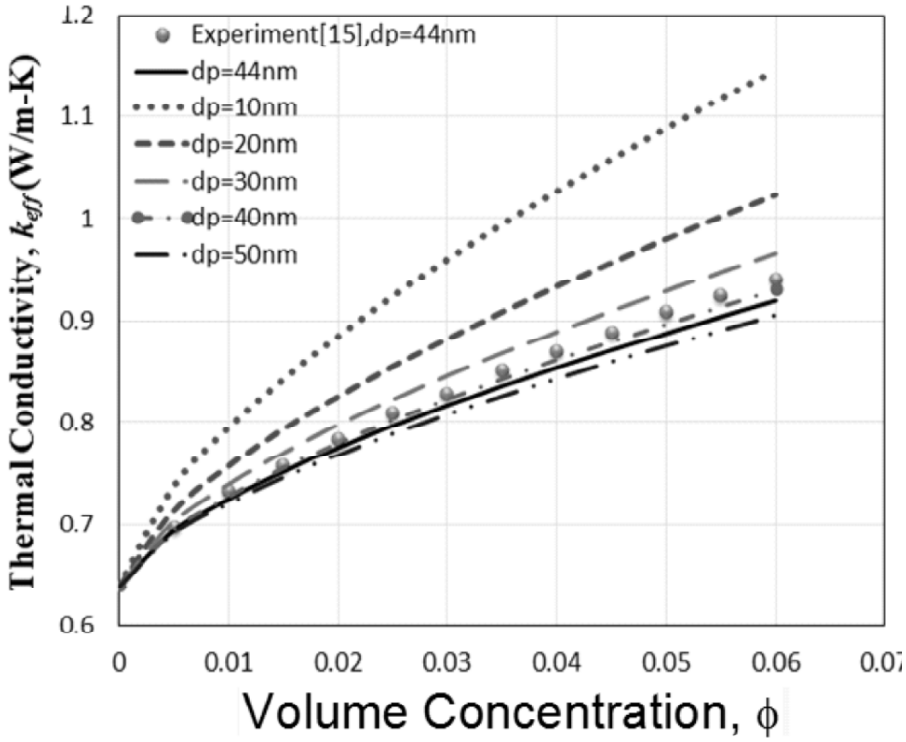

Figure 4: Thermal conductivity, k_{eff} $(W/m-K)$ of Al_2O_3-water nanofluids with volume concentration, ϕ at 50°C for the specified nanoparticle diameter (d_p)

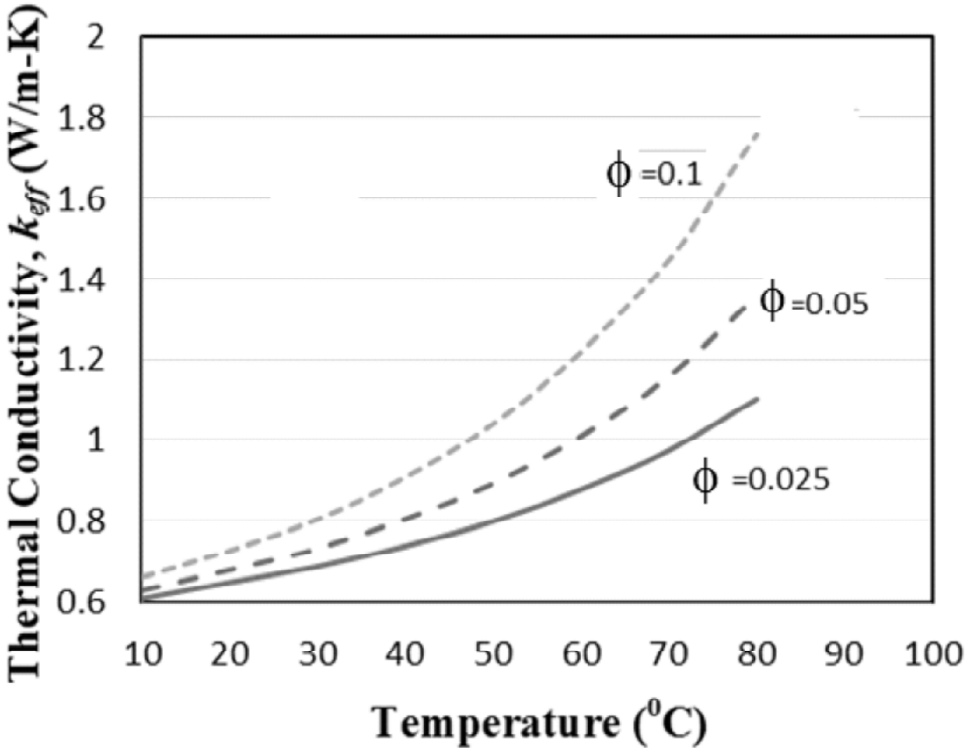

Figure 5: Variation of thermal conductivity, k_{eff} $(W/m-K)$ of Al_2O_3-water nanofluids with temperature (^{0}C) for the specified volume concentration, ϕ

$$\frac{\mu_{eff}}{\mu_f} = \left(1 - \alpha * 34.87 \left(\frac{d_p}{d_f}\right)^{-0.3} (\phi)^{1.03}\right)^{-1} \tag{22}$$

The modified Corcione empirical relation (22) with the multiplication factor, α = 0.775, the effective dynamic viscosity values are found to be reasonably in good agreement with test results (see Figure 6). The modified Corcione empirical relation (22) is considered for the effective dynamic viscosity evaluation at the specified temperatures volume concentration. These proposed equations are used to find out thermal properties of the Al_2O_3-water nanofluids for volume concentrations ϕ = 0.02, 0.03 and 0.04. Table 5 shows the comparison of properties generated from the empirical relations with test results [18] for 270C. An abrupt change is noticed in the measured viscosity values using a viscometer [18]. However the measured viscosity values at 50 °C are comparable with those generated from the modified Corcione empirical relation (22). Figure 7 shows the effect of nanoparticle diameter on dynamic viscosity. Figure 8 shows decrease in μ_{eff} with increasing temperature. Tables 6 to 8 provide thermal properties of the Al_2O_3-water nanofluids for volume concentration ϕ = 0.025, 0.05 and 0.1.

Table 5
Comparison of estimated properties of Al_2O_3–water nanofluids with test data at 27^{0}C

ϕ	ρ_{nf} (kg/m^3) Eq.(3)	C_{pnf} (kJ/kg.K) Eq.(4)	k_{eff} (W/m-K) Eq.(10)	μ_{eff} ($\times 10^{-4}$) (kg/m.s) Eq.(22)
0	996	4180	0.615	7.98
0.02	1055(1005)†	3923(4039)†	0.681 (0.625)†	9.03(2.2)†
0.03	1084(1050)†	3805(3910)†	0.701 (0.643)†	9.69(2.9)†
0.04	1114(1110)†	3693(3430)†	0.711 (0.662)†	10.47(7.5)†

†Test Results[18]

Table 6
Properties of Al_2O_3–water nanofluids at specified temperatures for ϕ = 0.025

Properties	*T=60^{0}C*	*T=70^{0}C*	*T=80^{0}C*
Thermal conductivity, k_{eff} (W/m-K)	0.8797	0.9765	1.1053
Specific heat, (kJ/kg.K)	3.8268	3.8666	3.8704
Density, ρ_{nf} (kg/m^3)	1060	1054	1049
Viscosity, μ_{eff} ($\times 10^{-4}$) (kg/m-s)	5.518	4.832	4.155
Prandtl number, Pr_{nf}	3.224	2.792	2.371

Table 7
Properties ofAl_2O_3 –water nanofluid at specified temperatures for ϕ = 0.05

Properties	*T=60^{0}C*	*T=70^{0}C*	*T=80^{0}C*
Thermal conductivity, k_{eff} (W/m-K)	1.0122	1.1602	1.3586
Specific heat, (kJ/kg.K)	3.5848	3.5891	3.5870
Density, ρ_{nf} (kg/m^3)	1134	1129	1124
Viscosity, μ_{eff} ($\times 10^{-4}$) (kg/m-s)	6.724	5.893	5.063
Prandtl number, Pr_{nf}	3.828	3.316	2.816

Table 8
Properties of Al_2O_3–water nanofluid at specified temperatures for $\phi = 0.1$

Properties	*T=60^{0}C*	*T=70^{0}C*	*T=80^{0}C*
Thermal conductivity, k_{eff}(W/m-K)	1.122	1.4503	1.7588
Specific heat, (kJ/kg.K)	3.1257	3.1259	3.1258
Density, ρ_{nf}(kg/m^3)	1284	1279	1274
Viscosity, μ_{eff}($\times 10^{-4}$) (kg/m-s)	12.146	10.644	9.145
Prandtl number, Pr_{nf}	6.708	5.811	4.935

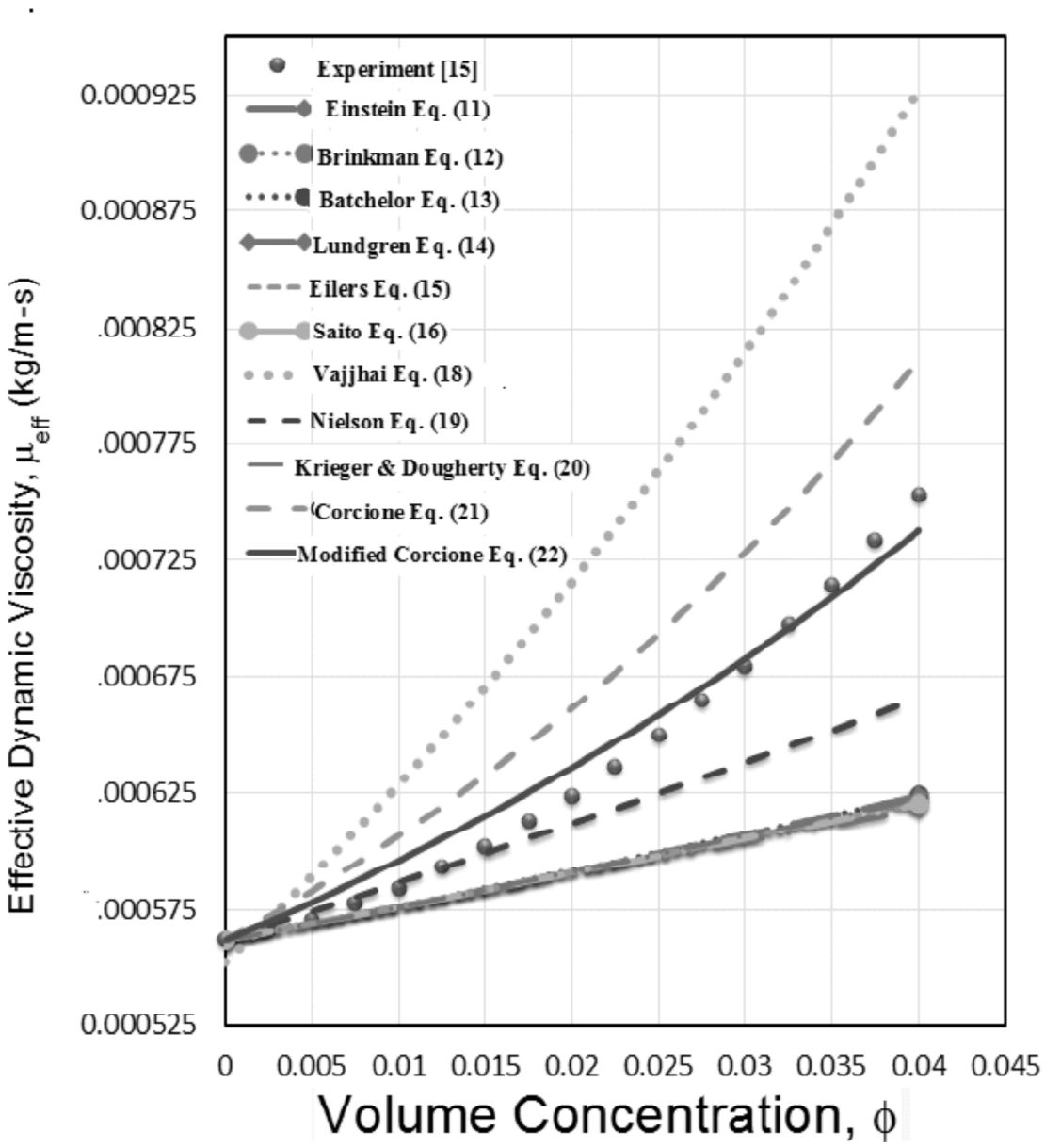

Figure 6: Comparison of effective dynamic viscosity, μ_{eff} (kg/m-s) of Al_2O_3-water nanofluids with volume concentration, ϕ

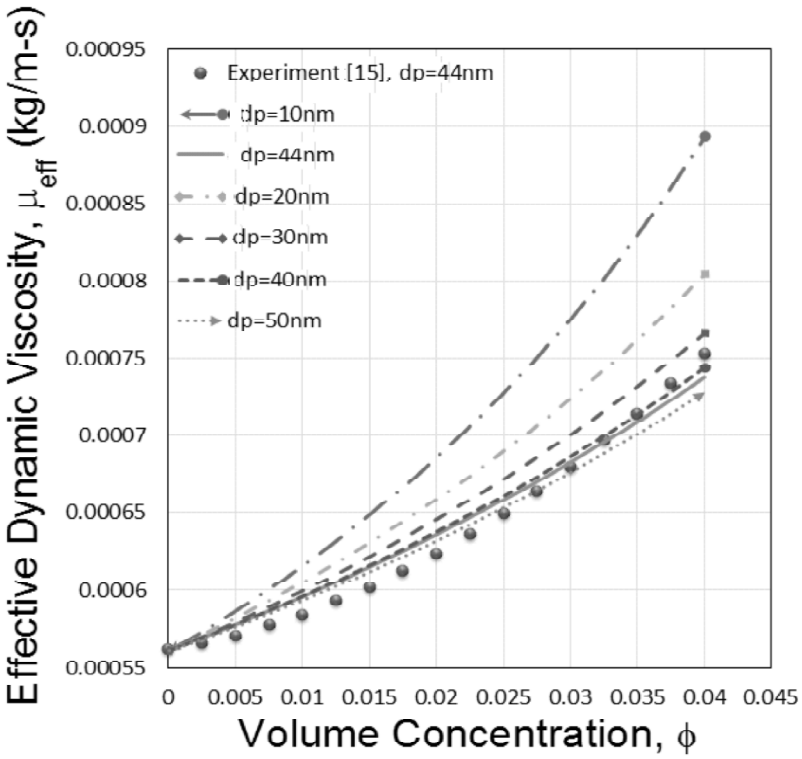

Figure 7: Effective dynamic viscosity, μ_{eff} (kg/m-s) of Al_2O_3-water nanofluids with volume concentration, ϕ at 50°C for the specified nanoparticle diameter (d_p) using the modified Corcione empirical relation (22)

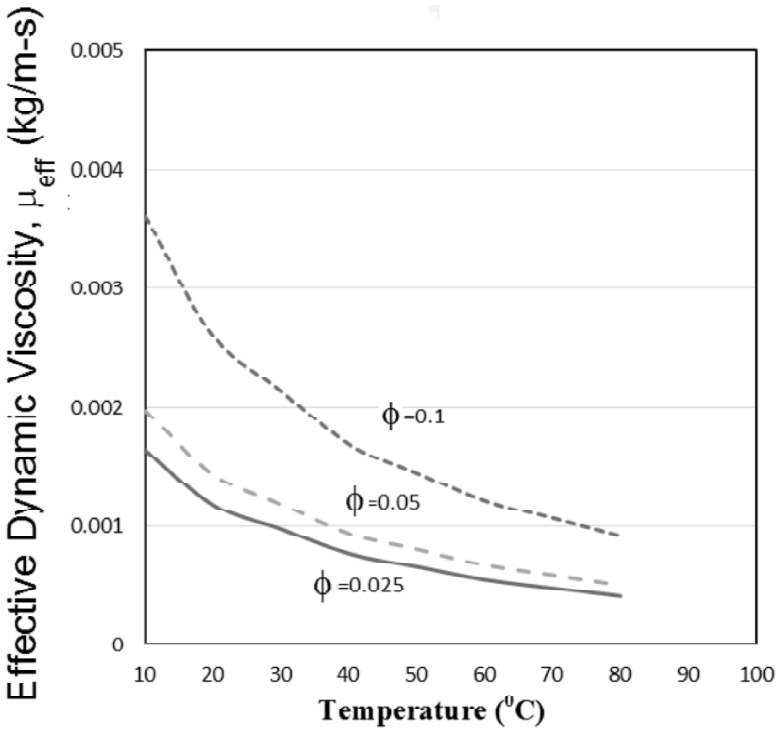

Figure 8: Variation of dynamic viscosity, μ_{eff} (kg/m-s) of Al_2O_3-water nanofluids with temperature (^{0}C) for the specified volume concentration, ϕ

4. HEAT TRANSFER ENHANCEMENT WITH Al_2O_3-WATER NANOFLUIDS

The most versatile shell- and- tube heat exchangers are used in process industries. They are also used as condensers (in conventional and nuclear power stations), and steam generators (in pressurized water reactor power plants). The major components in them are tubes, shell, frontend head, rear-end head, baffles, and tube sheets (Figure 9). They are built of round tubes mounted in a cylindrical shell with the tubes parallel to the shell. One fluid flows inside tubes, while the other fluid flows across and along the axis of the exchanger. The shell-and-tube heat exchangers provide relatively large ratios of heat transfer area to volume and weight, which can be designed for high-pressures relative to the environment and high-pressure differences between the fluid streams [16].

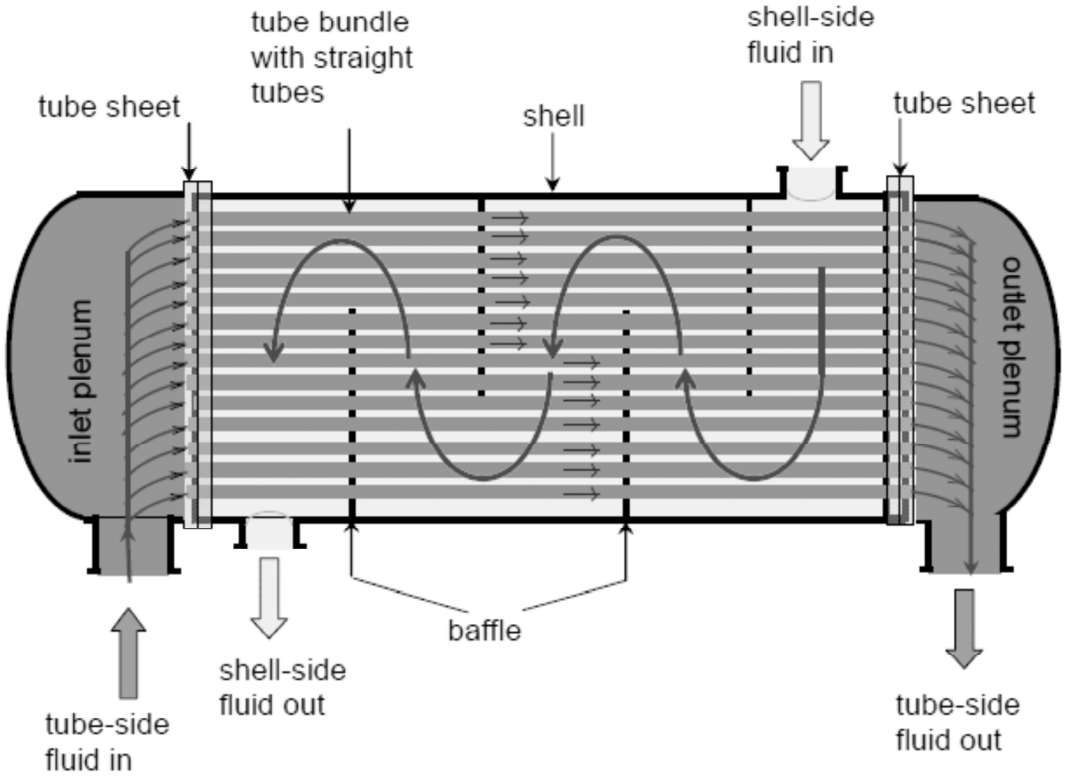

Figure 9: Straight Tube Heat Exchanger (One Pass Tube-Side: Countercurrent Flow) [16]

In order to find the outlet temperatures of cold and hot fluids there is a need to estimate effectiveness (ε), which is the ratio of actual heat transfer (Q) to the maximum possible heat transfer(Q_{max})). It signifies how efficiency of the heat exchanger is capable of transferring heat from hot fluid to cold fluid. Effectiveness is defined as

$$\varepsilon = \frac{Q}{Q_{\max}} \tag{23}$$

For counter-flow arrangement, the effectiveness (ε) in terms of NTU is

$$\varepsilon = \frac{e^{N(1-C)} - 1}{e^{N(1-C)} - C} \tag{24}$$

where, $N = \frac{UA}{C_{\min}}$, is the number of transfer units; $C = \frac{C_{\min}}{C_{\max}}$, is the capacity ratio; U is the overall heat transfer coefficient; A is the area to accommodate the number of tubes (N_t); $C_{min} = C_c = m_c C_{p_c}$) is the heat capacity of cold fluid; $C_{max} = C_h = m_h C_{ph}$, is the heat capacity of hot fluid. From equation (24) one can use ε and also evaluate maximum possible heat transfer Q_{max} from

$$Q_{max} = m_c C_{p_c}) (T_{hi}\text{-}T_{ci}), \tag{25}$$

where, m_h is the mass flow rate of hot fluid; C_{ph} is the specific heat of hot fluid; T_{hi} is the hot inlet temperature; T_{ci} is the cold inlet temperature.

Substituting ε and Q_{max} in equation (23) one gets the value of actual heat transfer (Q) and the outlet temperature of the hot fluid is obtained from

$$Q = m_h C_{ph}(T_{hi} - T_{ho}) \Rightarrow T_{ho} = T_{hi} - \left(\frac{Q}{m_h C_{ph}}\right) \tag{26}$$

In a similar way the outlet temperature of cold fluid is estimated from

$$Q = m_c C_{pc}(T_{co} - T_{ci}) \Rightarrow T_{co} = T_{ci} + \left(\frac{Q}{m_c C_{pc}}\right) \tag{27}$$

Heat transfer coefficient (hs) for shell side,

$$h_s = 0.37\,\mathrm{Re}_S^{-0.395}\, C_{p_S}\left(\frac{\dot{m}_S}{A_S}\right)\left(\frac{k_S}{C_{p_S}\mu_S}\right)^{0.66} \tag{28}$$

Here, $\mathrm{Re}_s = \frac{d_o \dot{m}_S}{\mu_S A_S}$, is the Reynolds number for shell side, which is a function of the tube outside diameter (d_o), mass flow rate of cold fluid in shell ($\dot{m}_s$),dynamic viscosity of cold fluid (μ_s), and the cross flow area of the shell (A_s); C_{ps} is the specific heat of cold fluid; and k_s is the thermal conductivity of cold fluid.

The heat transfer coefficient (h_t) for the tube side [17]

$$h_t = Nu_t \frac{k}{d_i}, \tag{29}$$

Here, k is the thermal conductivity of the tube material, d_i is the inside diameter of the tube, and the Nusselt number,

$$Nu_t = \frac{\left(\frac{f}{2}\right)\mathrm{Re}_t\,\mathrm{Pr}_t}{1.07 + 12.7\sqrt{\frac{f}{2}}(\mathrm{Pr}_t^{0.66} - 1)} \tag{30}$$

where, the Reynolds number for tube side,

$$\mathrm{Re}_t = \frac{\rho u_m d_i}{\mu}, \tag{31}$$

u_m is the average flow velocity in the tube, ρ and μ are the density and dynamic viscosity of the hot fluid in the tube. Pr_t is the prandtl number. The friction factor, $f = (1.58 \ln Re_t - 3.28)^{-2}$.

The overall heat transfer coefficient (U_c) is obtained from

$$\frac{1}{U_C} = \frac{1}{h_S} + \frac{d_0}{h_t d_i} + \frac{d_o}{2k} \ln\left(\frac{d_o}{d_i}\right) \tag{32}$$

The total pressure drop (Δp_s) over the shell side of the heat exchanger is

$$\Delta p_s = [0.24(N_b - 1)\Delta p_{bi} + 0.4 N_b \Delta p_{wi}] + 1.2\left(1 + \frac{N_{cw}}{N_c}\right)\Delta p_{bi} \tag{33}$$

Here $\Delta p_{bi} = 1.564(\mathrm{Re}_S)^{-0.148}\left(\frac{\dot{m}_S}{A_S}\right)^2\left(\frac{1}{2\rho_S}\right)N_C$; $\Delta p_{wi} = \frac{\dot{m}_S^2(2 + 0.6N_{cw})}{2\rho A_S A_w}$; N_b is the number of baffles; A_w is the area of the baffle window; N_c is the number of tube rows in a cross-flow section; N_{cw} is the number of effective cross-flow rows in each window.

Thermal and hydraulic analysis of the heat-exchanger has been carried out considering the cold fluid in shell as water and hot fluids in tubes as Al_2O_3-water nanofluids. In order to examine the heat transfer enhancement with the prepared Al_2O_3-water nanofluids, a typical shell and tube heat exchanger (preferring a single shell and single tube pass) shown in Figure 9 is considered. Input parameters to carry out the thermal-hydraulic analysis of the heat exchanger are: Shell inside diameter, D_s = 0.58m; Number of tubes, N_t = 374; Tube outside diameter, d_o = 19mm; Tube inside diameter, d_i = 16mm; Square tube pitch, P_T = 0.0254m; Baffle spacing, B = 0.5m; Cross flow area of the shell diameter, $A_S = D_S\left(1 - \frac{d_o}{p_T}\right) = 0.073m^2$; Temperature of raw water (cold fluid) in the shell = 30 °C; Temperature of hot water (hot nanofluid) in the tube = 60 °C, 70 °C, and 80 °C; Mass flow rate of cold fluid in shell, $\dot{m}$ =50kg/s; Mass flow rate of hot fluid in tube, $\dot{m}_t$ = 150kg/s; Thermal conductivity of tube material, k=42.3W/m.K; Average flow velocity in the tube, u_m = 2m/s; Length of the heat exchanger, L = 5m; Number of baffles, N_b = 9; Number of effective cross flow rows in each windows, N_{cw} = 5; Number of tube rows crossed in one cross flow section, N_c = 12; and Area of the baffle window, A_w = 0.076m2.

Properties of hot and cold fluids are given in Tables 1, 6 to 8. Analysis results are presented in Table 9. It can be observed from the results of Table 9 that the overall heat transfer coefficient enhances with Al_2O_3-water nanofluids. The effectiveness of shell and tube heat exchanger on energy basis is found to vary from 70.86% to 71.53% for water-water, whereas it varies from 75% to 83% for water-nanofluid for the specified volume concentrations and temperatures. Figures 10 and11 show the variation of tube side heat transfer coefficient and overall heat transfer coefficient with volume concentration(ϕ) varying from 0 to 0.1. The overall heat transfer coefficient increases with increasing ϕ up to 0.05 and decreases with further increasing ϕ up to 0.1. This clearly indicates that volume concentration should be limited to 0.05. The estimated pressure drop at shell side for the specified volume concentrations (0.025, 0.05 and 0.1) are 7.22, 7.21 and 7.19 kPa respectively. Table 10 gives the estimation of outlet temperatures of cold and hot fluids in the heat exchanger for the specified inlet temperatures directly from the ε-NTU method. As expected, the outlet temperature of hot fluid is less when compared to that

Table 9
Thermal analysis results of a heat exchanger with cold fluid (water) and hot fluid (Al_2O_3-water nanofluid) at the specified temperatures (viz., Nusselt number, Nu_t; Shell side heat transfer coefficient, h_s (W/m²K); Tube side heat transfer coefficient, h_t (W/m²K); Overall heat transfer coefficient, U_c (W/m²K); and Effectiveness, ε)

T_{hi} (°C)	ϕ	Re_t Eq. (31)	Nu_t Eq. (30)	h_s Eq. (28)	h_t Eq. (29)	Uc Eq. (32)	ε (%) Eq. (24)
60	0	66945	282.6	4399.5	11503.9	2709.2	70.86
	0.025	61441	236.5	4399.5	13005.6	2799.7	75.22
	0.05	53971	211.1	4399.5	13350.7	2818.3	77.79
	0.1	33813	165.1	4399.5	12602.8	2777	82.05
70	0	75952	291.6	4399.5	12030.6	2742.8	71.20
	0.025	69757	231.1	4399.5	14104.4	2856.8	75.47
	0.05	61304	202.7	4399.5	14698.2	2884.6	78.45
	0.1	38437	157.5	4399.5	14276.3	2864.8	82.92
80	0	87921	301.1	4399.5	12584.4	2775.8	71.53
	0.025	80777	222.6	4399.5	15378.1	2919.6	76.06
	0.05	71022	191.3	4399.5	16247.1	2950.1	79.14
	0.1	44563	147.7	4399.5	16239.3	2949.8	83.72

Table 10
Estimated outlet temperatures of cold and hot fluids in the heat exchanger

Specified Inlet Temperatures (°C)		*Estimated Outlet Temperatures (°C)*	
T_{hi}	T_{ci}	T_{ho}	T_{co}
		$\phi = 0$	
60	30	38.74	37.09
70	30	48.63	37.13
80	30	58.53	37.18
		$\phi = 0.025$	
60	30	37.43	36.89
70	30	47.35	36.98
80	30	57.18	37.04
		$\phi = 0.05$	
60	30	36.66	36.67
70	30	46.46	36.73
80	30	56.25	36.79
		$\phi = 0.1$	
60	30	35.38	36.13
70	30	45.12	36.20
80	30	54.88	36.26

of inlet temperature, whereas the outlet temperature of the cold fluid is high when compared to that of inlet temperature. The outlet temperatures of cold and hot fluids are found to decrease with increasing volume concentration.

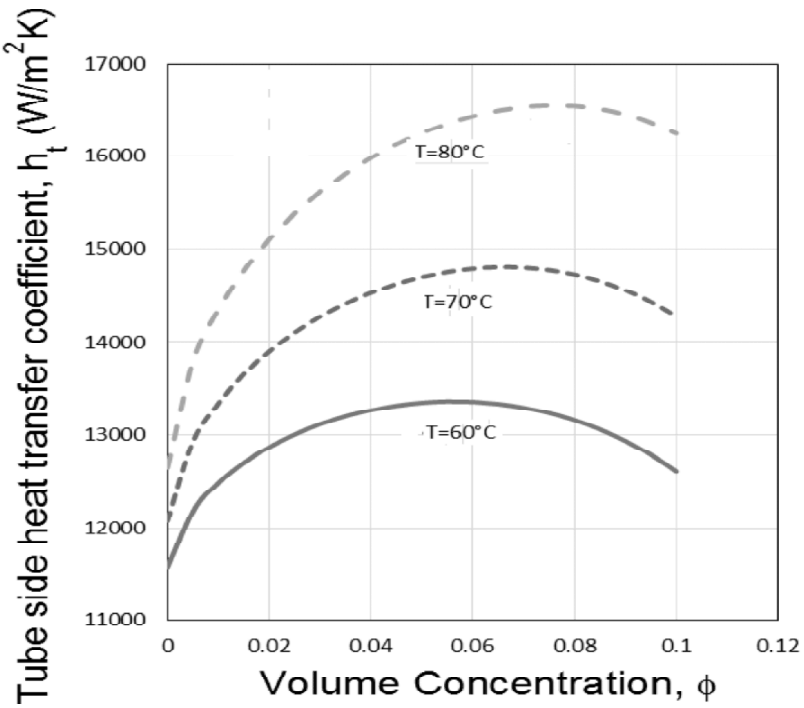

Figure 10: Variation of the tube side heat transfer coefficient, h_t (W/m²K) with volume concentration, ϕ

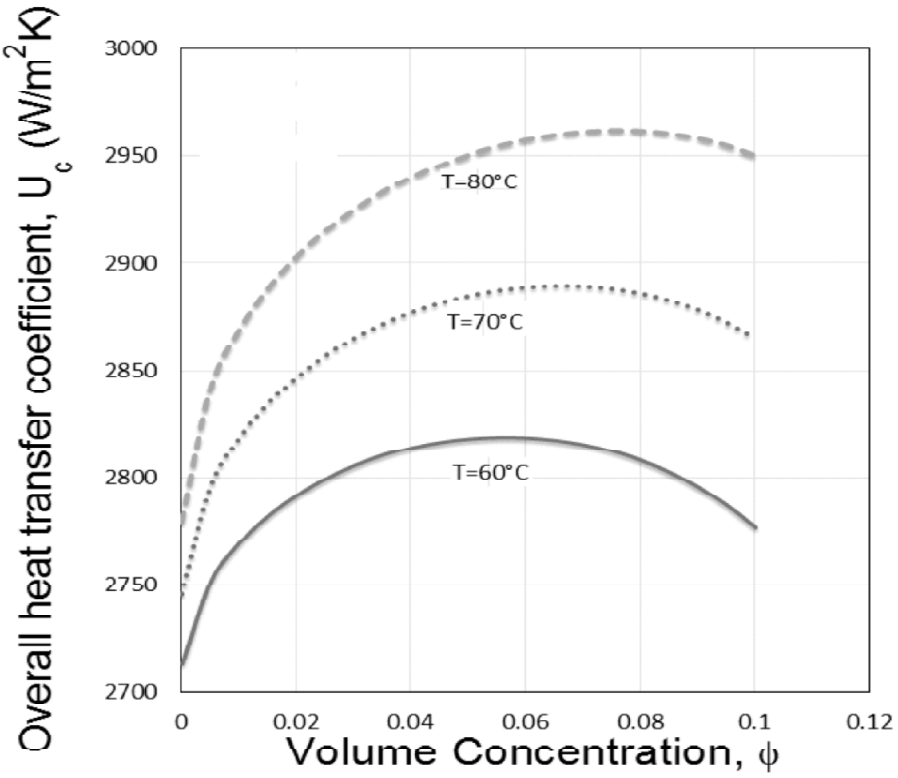

Figure 11: Variation of the overall heat transfer coefficient, U (W/m²K) with volume concentration, ϕ

5. CONCLUDING REMARKS

This paper presents briefly on the preparation of Al_2O_3-water nanofluids and their properties (viz., density, specific heat, viscosity, and thermal conductivity) for the specified volume concentration and temperature. The thermo physical properties of nanofluid measured at 50 ^{0}C are compared with several empirical models and selected Corcione model as the best suited model. A typical shell and tube heat exchanger is considered to examine the heat transfer characteristics by using water and nanofluid as working fluids. When the heat exchanger runs with water as working fluid, overall heat transfer coefficient improved with increase in the water inlet temperature. On the other hand it is decreased with increasing volume concentration when nanofluid is used as a working fluid. The Reynolds number and Nusselt number are decreased with increasing in volume concentration. The overall heat transfer coefficient is found to increase for the specified inlet temperatures (from 60 to 80^{0}C), but there is a moderate change occurred due to volume concentration. The overall heat transfer coefficient for Al_2O_3 nanofluid to water is higher for volume concentration, $\phi = 0.025$ at different temperatures (ranges from 60 to 80^{0}C).As the volume concentration increases, a little reduction in the enhancement is noticed. The enhancement in overall heat transfer coefficient for the specified volume concentration, $\phi = 0.025$, 0.05 and 0.1 are 7.58%, 7.55% and 6.26% respectively when the inlet temperature of the nanofluid is 80^{0}C.

REFERENCES

[1] Lee S., Choi S.U.S., Li S. and Eastman J.A., "Measuring thermal conductivity offluids containing oxide nanoparticles", *Trans. ASME J. Heat Transf.,* **121**(2), 280–289 **(1999)**.

[2] Das S.K., Putta N., Thiesen P. and RoetzelW.,"Temperature dependence of thermal conductivity enhancement for nanofluids",*J. Heat Transf.*, **125** (4), 567–74 **(2003)**.

[3] Xuan Y., Li Q., Zhang X. and FujiiM.,"Stochastic thermal transport of Nanoparticle suspensions", *J.Appl. Phys.*,**100**(4), 043507 **(2006)**.

[4] Ebrahimi M., Farhadi M., Sedighi K., and Akbarzade S., "Experimental investigation of force convection heat transfer in a car radiator filled with SiO_2-water nanofluid", IJE Transactions B: Applications, **27** (2), 333-340 **(2014)**.

[5] Khanfer K. andVafai K., "A critical synthesis of thermo physical characteristics of nanofluids",*International Journal of Heat and Mass Transfer*.**54**,4410-4428 **(2011).**

[6] Xuan Y., Li Q. and Hu W., "Aggregation structure and thermal conductivity of nanofluids", *AIChE,* **49**(4), 1038–1043 **(2003)**.

[7] Corcione M., "Empirical correlating equations for predicting the effective thermal conductivity and dynamic viscosity of nanofluids", *Ene. Convers. Manage.*,**52**(1), 789-793 **(2011)**.

[8] Pak B.C.andCho Y.I., "Hydrodynamic andheat transfer study of dispersed fluids with submicron metallic oxide particles", *Exp.Heat. Transf.*, **11**(2), 151-170 **(1998)**.

[9] Kakaç, S. and Pramuanjaroenkij, A., "Review of convective heat transfer enhancement with nanofluids", International Journal of Heat and Mass Transfer, **52**(13), 3187- 3196 **(2009).**

[10] Masuda H., Ebata A., Teramae K. and Hishinuma N., "Alteration of thermal conductivity and viscosity of liquid bydispersing ultra-fine particles" (dispersion of ãAl2O3, SiO2, and TiO2 ultra-fine particles), *Netsu. Bussei.*,**4**(4), 227–233 **(1993)**.

[11] Murshed S.M.S., Leong K.C. and Yang C., "Investigations of thermal conductivity and viscosity of nanofluids",*Int. J. ThermalSci.*, **47** (5), 560-568 **(2008)**.

[12] Putra N., Roetzel W. and Das S.K., "Natural convection of nanofluids", *J. Heat.Mass. Transf.*,**39**(9)**,** 775-784 **(2003)**.

[13] Nguyen C.T., Desgranges F., Galanis N.R.G., Mare T.B.S. and AngueMintsa H., "Viscosity data for Al_2O_3-water-nanofluid-hysteresis:Isheattransfer enhancement usingnanofluids reliable?",*Int. J. Therm.Sci.*, **47** (2), 103-111**(2008)**.

[14] Vajjha R.S., Das D.K., Namburu P.K., "Numerical study of fluid dynamic and heat transfer performance of $Al_2O_3$and CuOnanofluidsin theflat tubes of raditor", *Int. J. Heat and Fluid Flow,***31**, 613-621 **(2010).**

[15] Tiwari A.K., Pradyumna G. and Jahar S., "Investigation of thermal conductivity and viscosity of Al_2O_3-water nanofluid",*J Environ Res. Develop*., **7** (2), 768-777 **(2012).**

[16] Kakac S. and Liu H., "Heat Exchangers Selection Rating and Thermal Design", Second Edition; Chapter 8, pp.300-326 **(2002).**

[17] Petkov B. S., "Heat transfer and friction in turbulent pipe flow with variable physical properties", In Advances in Heat Transfer, (Editors: J.P. Hartnett and T.V. Irvine) Academic Press, New York **(1970).**

[18] Pandey S.D. and NemaV.K.,"Experimentalanalysis of heat transfer and friction factor of nanofluid as a coolant in a corrugated plate heat exchanger",*ExperimentalThermal and Fluid Sciences*, **38**,248-256 **(2012).**